Pulsed Electroplating of Metal Nanoparticles form DODUCO Electrolytes

Eduard MONAICO[1*], Oana BRINCOVEANU[2], Raluca MESTERCA[2], Veaceslav URSAKI[3], Mariana PRODANA[2], Marius ENACHESCU[2], Ion TIGINYANU[1,3]
[1]*National Center for Material Study and Testing, Technical University of Moldova*
[2]*Center for Surface Science and NanoTechnology, University Politehnica of Bucharest*
[3]*Institute of Electronic Engineering and Nanotechnologies, Academy of Sciences of Moldova*
**m_eduard_y@yahoo.com*

***Abstract* — The mechanisms of Au deposition on InP porous substrates during a pulsed electroplating process are investigated by means of Topography imaging and Current Mapping measurements. The obtained results confirm the formation of Schottky barriers at the interface of the semiconductor substrate with Au nanoparticles with diameters around 20 nm, and corroborate the hypothesis that the mechanism of Au nanoparticles self-assembling into monolayers is governed by the formation of such Schottky barriers. The analysis of current-voltage curves suggest also the deposition of a dielectric film over the larger Au particles produced with long duration pulsed electroplating from DODUCO solutions.**

***Index Terms* — Semiconductor substrate, electroplating, Atomic force topography, Current mapping.**

I. INTRODUCTION

Nanoparticles (NPs), including metallic ones, are important building blocks of a variety of nanodevices and smart materials. Techniques for assembling and organizing nanoparticles into controlled architecture starting from arrays and monolayers to complex 3D architectures are under development.

The colloidal approach in assembling complex nanoparticle structures via their immobilization on solid substrates for the construction of functional interfaces and their application in a variety of electronic, optical and sensor components has been previously reviewed [1]. Sol–gel processes, hydrothermal and homogenous precipitation, reverse micelles method, chemical reduction technique, and radio-frequency co-sputtering techniques are also widely used for the synthesis of nanometric metal particles (see, for instance, review [2] and refs therein).

Among other technologies, for conducting supports, electrodeposition is especially attractive, since it provides electrical connection of NPs arrays to the substrate, and it does not need stabilizing surfactants, which impacts the NP surface chemistry [2,3]. Apart from that, the size, shape, composition, and spatial distribution of NPs are easily controlled by tuning the deposition parameters and electrolyte composition. The method is simple, fast, and inexpensive, highly stable and reproducible. Electrodeposition has been applied for deposition of metal nanoparticles on a variety of substrates and templates, such as silicon [3], stainless steel [4], indium tin oxide (ITO) coated glass [2], porous silicon [5], nanoporous anodic alumina oxide (AAO) [2], wide-band gap metal oxide nanostructured substrates [6,7], and a variety of carbonic materials, such as glassy carbon electrode [2], highly oriented pyrolytic graphite (HOPG) [8], carbon sphere surfaces [9], carbon nanotubes (CNT) [10,11], graphite nanofibers (GNFs), carbon nanohorns, and carbon nanocoils [12], graphene and graphene oxide [13,14].

The mechanisms of metal nanoparticles self-assembling into nanoparticle layers and films during electrodeposition are quite complex. Particularly, it was proposed to functionalize the surface of metal nanoparticles with multiple redox species, biferrocene (BFc) or anthraquinone (AQ) thiol derivatives, in order to control the deposition mechanism [15].

The possibility to cover the surface of InP and GaP porous structures by a self-assembled monolayer of electrochemically deposited nanoscale Au nanodots have been recently demonstrated by applying pulsed electroplating [16]. The mechanism of self-assembling was suggested to be governed by the formation of Schottky barriers at the interface between the porous semiconductor surface and the Au dots. It was found in a previous research that the value of the Schottky barrier height depends on the size of the metallic dots [17]. For instance, the surface barrier height at a Pt dot rapidly increases toward the value of the Mott-Schottky limit of 1.1 eV as the Pt dot diameter decreases to approx. 23 nm. Therefore, it was supposed that the metal deposition conditions on porous semiconductor templates change with changing the diameters of metal nanoparticles, which leads to a kind of hopping process: metal deposition "jumps" from one local area to other ones as soon as one or more dots reach the threshold value of the diameter. This process continues until the entire surface exposed to the electrolyte is covered by a monolayer of metallic nanoparticles.

The goal of this paper is to investigate by means of Current Mapping in an Atomic Force Microscope (AFM) the evolution of Schottky barriers at the interface between the porous semiconductor surface and the Au nanoparticles deposited by pulsed electroplating.

II. Description of Technological Procedures

Crystalline 500-µm thick n-InP(100) substrates with the free electron concentration of $1.3x10^{18}$ cm^{-3} supplied by CrysTec GmbH were subjected to anodic etching in 500 ml of 5% HCl aqueous solution at 25°C to fabricate porous layers as described elsewhere [18].

Electroplating of Au was realized at 25°C in a common two-electrode plating cell with commercially available gold or silver baths (DODUCO) where the porous sample served as working electrode, while a platinum wire was used as counter electrode. A pulsed voltage with pulse duration of 100 µs and a cathodic voltage of -16 V was applied between the two electrodes to electrochemically reduce the metal species on the surface of the samples being in contact with the electrolyte. After each pulse, a delay time up to one second was kept. The solution was magnetically stirred to provide appropriate conditions for the recovery of the ion concentration in the electrolyte.

Both types of pores perpendicular and parallel to the substrate surface can be produced in the InP substrate. The ohmic contact is deposited on the opposite surface of the substrate with respect to the surface exposed to the electrolyte for production of pores perpendicular to the substrate surface. In such a case, the current oriented pores grow from the surface exposed to electrolyte in the direction of the ohmic contact.

For producing pores parallel to the substrate surface, a part of the front surface of the substrate is covered by a photoresist (region 2 in Fig. 1), and another part is exposed to the electrolyte in the electrochemical etching process (region 1). In this case, the pores grow from the surface exposed to the electrolyte initially in a direction perpendicular to the surface. However, with the further propagation of pores, they are deflected in a direction parallel to the surface and grow under the regions covered by the photoresist as shown in Fig. 1b. An interesting feature of porous structures obtained by this method is the production of buried porous layers. Actually, the buried pores grew under a 60-nm thick surface layer of virgin InP, which remains intact during the electrochemical treatment. This surface layer formed under the photoresist is transparent for electrons in a SEM instrument, and it can be removed chemically after the anodic etching. Metal nanoparticles can be deposited inside pores as described above. As one can see from Fig. 1c, the inner surface of pores is covered by a dens monolayer of Au dots with average size of 20 nm after electroplating by applying ten cathodic voltage pulses of 100 µs width as described above. The density of Au nanoparticles can be controlled by adjusting the voltage pulse width in the range of 1÷100 µs.

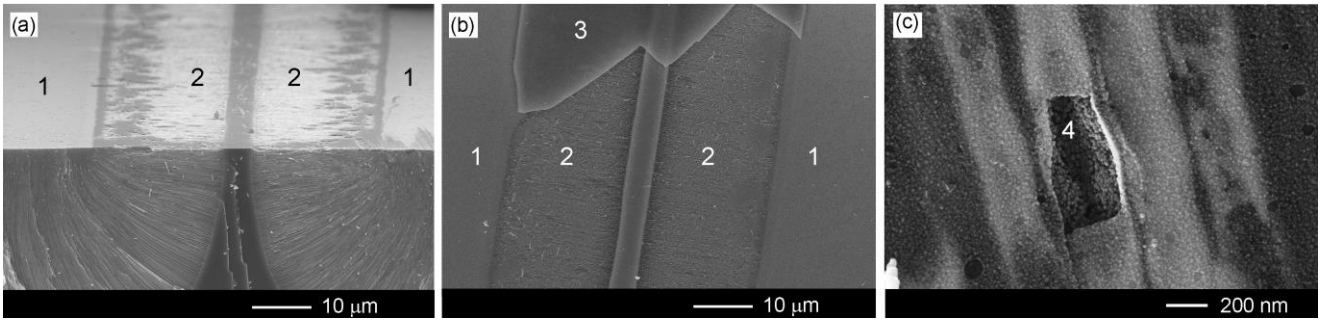

Fig. 1. (a) Cross section SEM view of a porous InP structure produced by anodic etching through windows produced by photolithography; (b) top view of the produced structure with a piece of the photoresist layer (region 3); (c) view of pores filled with a monolayer of Au dots with a piece of the surface layer being removed (region 4).

III. Topography Imaging and Current Mapping

Topography imaging and Point Contact Microsocpy (PCM) [19] measurements were performed in ambient atmosphere in contact mode using a silicon/Pt-coated cantilever with the spring constant of 0.11 N/m and 22 kHz resonance frequency. Simultaneous images of the sample topography and local current mapping using PCM were obtained, allowing to correlate localized current with sample features. A bias voltage V_{tip} of 5V was applied between the tip and sample surface. The measurements were carried on using a Solver Next (NT-MDT) AFM equipment. The samples were analyzed choosing two different scan areas: 10 µm × 10 µm and 5 µm × 5 µm.

The schematic representation of the circuit used for PCM implementation and current-voltage curve measuring is presented in Fig. 2.

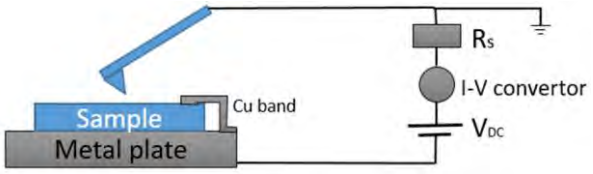

Fig. 2. Schematic representation of the circuit used for PCM implementation and current-voltage curve measuring.

In order to assess the potential barrier built up at the metal-semiconductor interface, a layer of Au nanoparticles of different thickness was electroplated on the surface of an InP sample with a buried porous structure. Fig. 3 illustrates the topography and current mapping images of such a layer. One can see that the morphology of the layer is non-uniform on different regions of the substrate. Most probably, the non-uniformity is due to the initial state of the substrate. Nevertheless, the reproducibility of the measurement is proved by the presence of the same features in both images (10 x 10 µm and 5 x 5 µm).

The analysis of Current Mapping images suggests the variation of the Au nanoparticle layer thickness over the substrate surface. The regions with red color (high current densities) correspond to a thin layer (a monolayer of Au nanoparticles with the size of around 20 nm) as described in the technology procedures section.

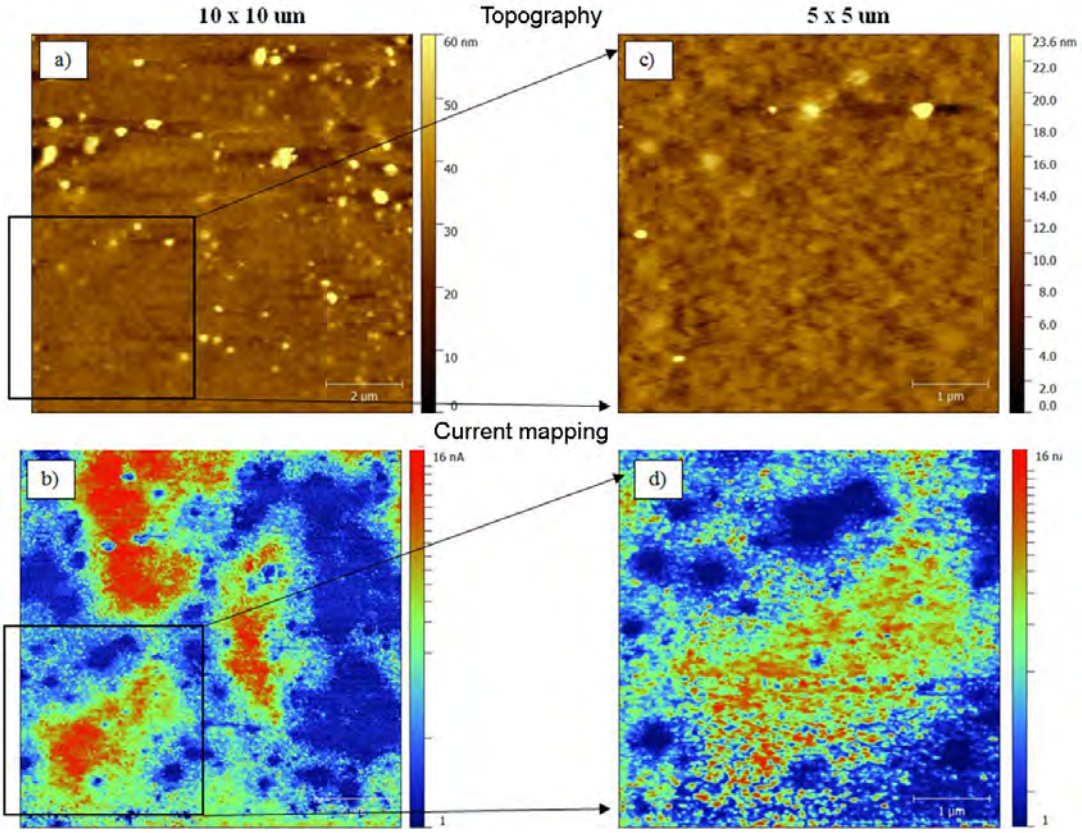

Fig. 3. Topography (a, c) and current mapping images (b, d) on 10 x 10 µm and 5 x 5 µm scan sizes; Images (c) and (d) correspond to a zoom-in scan in the 10x10 µm image.

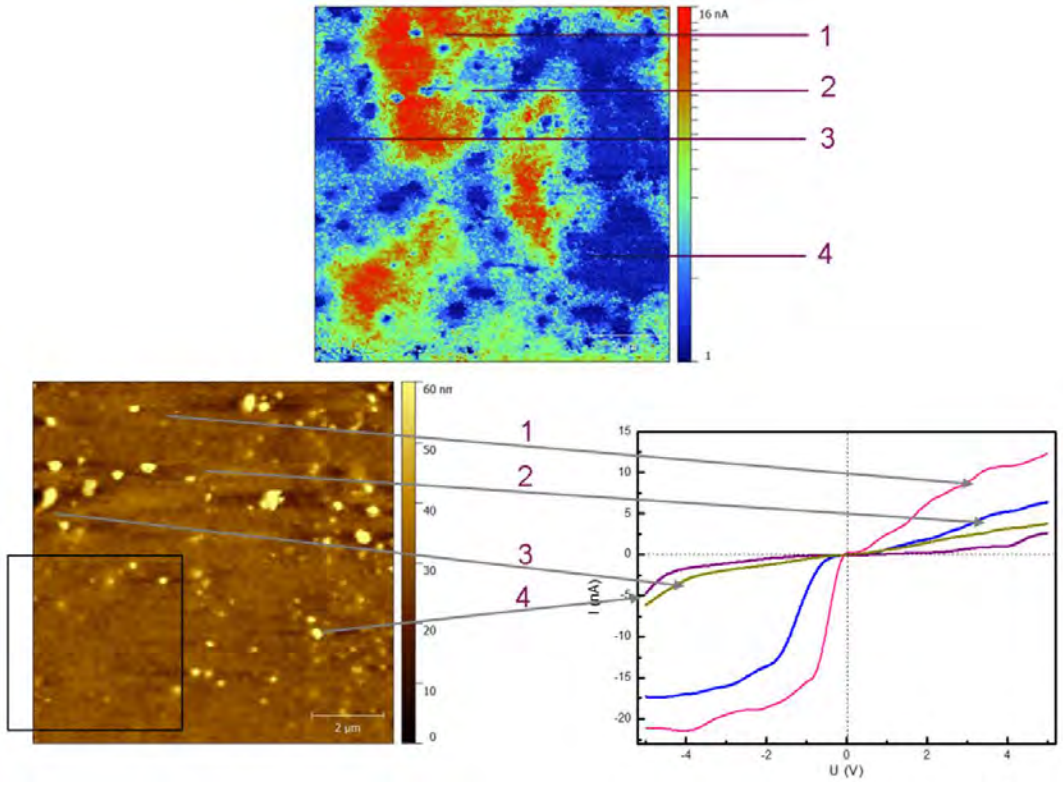

Fig. 4. I-V curves (right) acquired in the indicated spots on the topography, image (left), and current mapping image (up), of the sample, with a 10 x 10 µm scan size.

The regions with blue color in the Current Mapping images correspond to thicker Au layers formed from larger Au particles. Larger Au particles (with the size around 100-300 nm) are also deposited onto the regions with thin nanoparticles layers, indicated by blue circles in a red background.

The formation of Schottky barriers is indicated by the analysis of I-V curves in Fig. 4. Measurements in the point 1 in Fig. 4 with high value of the current demonstrate an I-V curve typical for Schottky diodes, which confirms deposition of a monolayer of Au nanoparticles. As discussed in the introduction section, the mechanism of self-assembling of metal nanoparticles in a monolayer is governed by the formation of Schottky barriers. The breakdown of the Schottky barrier at a voltage of 5 V at the cantilever tip leads to current flow in these regions, which produces a red color in the current mapping image.

The I-V curve in the point 2 with a yellow color in Fig. 4 suggests also the formation of a Schottky barrier, but with a higher breakdown voltage. One can suggest that a thin dielectric film is deposited on the metal nanoparticle layer, which leads to a lower current density in this point.

The I-V curves measured in regions with a thicker metal layer (point 3) or at a larger metal particle (point 4) in Fig. 4, with blue color, suggest that a thicker dielectric film is deposited over the metallic nanoparticle in these regions of the sample. This dielectric film prevents the current flow in these regions at an applied voltage of 5 V, which is not enough for the breakdown of the dielectric film.

These observations are also corroborated by the measurements performed with a 5 x 5 µm scan size (Fig. 5) in the region of a large metal particle (point1), a thick metal layer (point 2), and a thin (monolayer) of Au nanoparticles (point 3).

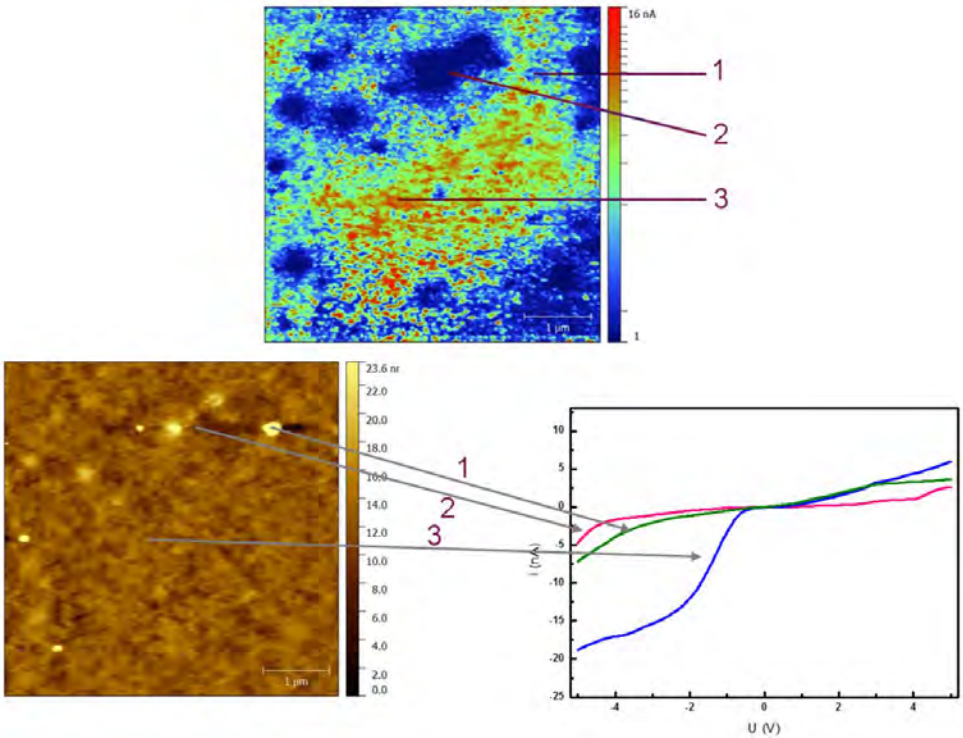

Fig. 5. I-V curves (right) acquired in the indicated spots on the topography, image (left), and current mapping, image (up), of the sample, with a 5 x 5 µm scan size.

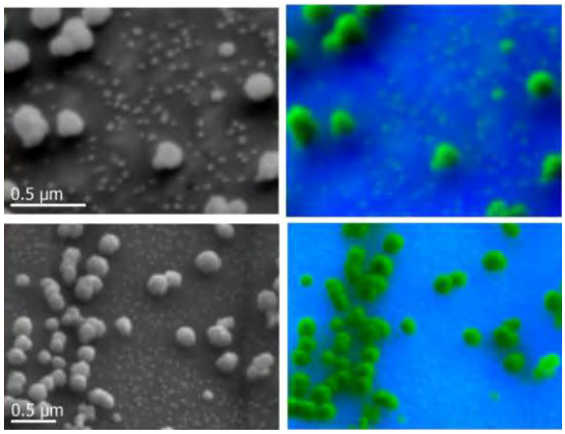

Fig. 6. (a) SEM images (left) and corresponding color-composite (380+525) nm CL images (right) of a ZnO sample with deposited Au nanoparticles.

The deposition of a dielectric film over metallic Au particles at long duration of pulsed electroplating is also confirmed by cathodoluminescence (CL) measurements on large Au particles (with diameter around 200 nm) electrodeposited on a ZnO substrate, illustrated in Fig. 6. One can see from the composite CL image, excited by a 10 kV, 10 nA electron beam, that the UV (380 nm) luminescence comes from the ZnO substrate, while an intense green (525 nm) luminescence is emitted by Au particles. The green luminescence can be produced neither by virgin Au particles, nor by the Au oxidation processes. Most likely, the green luminescence comes from a dielectric film deposited over the Au particles from the DODUCO solution.

IV. CONCLUSION

The results of this study demonstrate the formation of Schottky barriers at the interface of Au nanoparticles monolayer with the semiconductor substrate and suggest the deposition of a dielectric film over the larger Au particles produced with long duration pulsed electroplating.

ACKNOWLEDGMENTS

This work was supported financially by Academy of Sciences of Moldova under the grant No. 16.80013.5007.08/RO, by Romanian Ministry of Education and Scientific Research and by Executive Agency for Higher Education, Research, Development and Innovation, under Projects PCCA 66/2014 and ENIAC 04/2014.

REFERENCES

[1] A. N. Shipway, E. Katz, I. Willner, "Nanoparticle arrays on surfaces for electronic, optical, and sensor applications", ChemPhysChem, vol. 1, pp. 18-52, 2010.

[2] U. S. Mohanty, Electrodeposition: a versatile and inexpensive tool for the synthesis of nanoparticles, nanorods, nanowires, and nanoclusters of metals, J Appl Electrochem, vol. 41, pp. 257–270, 2011.

[3] G. Oskam, J. G. Long, A. Natarajan, P. C. Searson, Electrochemical deposition of metals onto silicon, J. Phys. D: Appl. Phys., vol. 31, pp. 1927–1949, 1998.

[4] H. Heydari, A. Abdolmaleki, M. B. Gholivand, H. Shayani-jam, Electrodeposition and characterization of palladium nanostructures on stainless steel and application as hydrogen sensor, Ciencia e Natura, Santa Maria, vol. 37, Part 1, pp. 23−33, 2015.

[5] E. Ko, J. Hwang, J. H. Kim, J. H. Lee, S.H. Lee, V.-K. Tran, W. S. Chang, C. H. Park, J. Choo, G. H. Seong, Electrochemical fabrication of nanostructures on porous silicon for biochemical sensing platforms, Analytical Sci. vol 32, pp. 681-686, 2016.

[6] M.A.K.L. Dissanayake, et al., Efficiency enhancement in plasmonic dye-sensitized solar cells with TiO_2 photoanodes incorporating gold and silver nanoparticles, J. Appl. Electrochem. vol. 46, pp. 47-58, 2015.

[7] T. Wang, et al., Vertically aligned ZnO nanowire arrays tip-grafted with silver nanoparticles for photoelectrochemical applications, Nanoscale, vol, 5, pp. 7552, 2013.

[8] S. C. S. Lai, R. A. Lazenby, P. M. Kirkman, P. R. Unwin, Nucleation, aggregative growth and detachment of metal nanoparticles during electrodeposition at electrode surfaces, Chem. Sci., vol. 6, 1126, 2015.

[9] M. A. Hassan, Z. A. Hamid, N. Nassif, M. Rabah, Electrodeposion of siver nanoparticles on cardon spheres surfaces by pulse current, Int. J. Tech. Res. Appl. vol. 2, pp. 154-158, 2014.

[10] S. Saipanya,.S. Lapanantnoppakhun, T. Sarakonsri, Electrochemical deposition of platinum and palladium on gold nanoparticles loaded carbon nanotube support for oxidation reactions in fuel cell, J. Chemistry, vol. 2014, pp. 104514, 2014.

[11] L. Li, L. Dai, Template-free electrodeposition of multicomponent metal nanoparticles for region-specific growth of interposed carbon nanotube micropatterns, Nanotechnology, vol. 16, pp. 2111–2117, 2005.

[12] Md. A. Islam, M. S. Islam, Electro-deposition method for platinum nanoparticles synthesis, Eng.Internat. vol. 1, pp. 9-18, 2013.

[13] I. Khalil, N. M. Julkapli, W. A. Yehye, W. J. Basirun, S. K. Bhargava, Graphene–gold nanoparticles hybrid—synthesis, functionalization, and application in a electrochemical and surface-enhanced raman scattering biosensor, Materials, vol. 9, pp. 406, 2016.

[14] Z. Yu, S. Sun, M. Huang, Electrodeposition of gold nanoparticles on electrochemically reduced graphene oxide for high performance supercapacitor electrode materials, Int. J. Electrochem. Sci., vol. 11, pp. 3643 – 3650, 2016.

[15] M.Yamada, H. Nishihara, Electrochemical deposition of metal nanoparticles functionalized with multiple redox molecules, Comptes Rendus Chimie, vol. 6, pp. 919-934, 2003.

[16] I. Tiginyanu, Ed. Monaico, K. Nielsch, Self-Assembled Monolayer of Au Nanodots Deposited on Porous Semiconductor Structures, ECS Electrochem. Lett., vol. 4, pp. D8-D10, 2015.

[17] H. Hasegawa and T. Sato, Electrochemical processes for formation, processing and gate control of III–V semiconductor nanostructures, Electrochimica Acta, 50, 3015-3027, (2005).

[18] E. Monaico, I. Tiginyanu, O. Volciuc, Th. Mehrtens, A. Rosenauer, J. Gutowski, K. Nielsch, Formation of InP nanomembranes and nanowires under fast anodic etching of bulk substrates, Electrochem. Commun., 47, 29 (2014).

[19] M. Enachescu, D. Schleef, D. F. Ogletree, and M. Salmeron, Integration of Point-Contact Microscopy and Atomic-Force Microscopy: Application to Characterization of Graphite/Pt(111), Phys. Rev. B, 60, 16913 (1999).